

Aperture synthesis in optical astronomy; the current status

Swapan K. Saha
Indian Institute of Astrophysics,
Bangalore - 560 034, India

Abstract

A milestone in observational astronomy was achieved when the interferometric fringes of α Lyrae (Vega) in the visible band were obtained in July 1974, by A. Labeyrie from an interferometer, called Interféromètre à deux télescope (I2T), with a pair of independent telescopes on a North-South baseline configuration at Nice Observatory. These were the first fringes that are obtained by using the concept of merging speckles from both the telescopes. Such a success in synthesizing images impelled astronomers to venture towards ground-based very large arrays. Potentials for progress in the direction of developing large interferometric arrays of telescopes are expected to provide images, spectra of quasar host galaxies, exo-planets that may be associated with stars outside our solar system. Several interferometers using large telescopes (8-10 meters) have been successfully producing results since the dawn of this century and several new such instruments will be in operation soon both at ground, as well as in space. In view of the present scenario the current trend and the path to future progress in optical interferometry using diluted apertures are discussed.

1 Introduction

The interferometry at optical wavelengths in astronomy began with Fizeau [1], but the field lay dormant after the measurement of the diameter of α Orionis by Michelson's stellar interferometer [2]. It was revitalized by the intensity interferometry [3] and the pioneer's era ended with the Narrabri intensity interferometer [4] by which 32 southern stars were resolved. The optical interferometric imaging, triggered in 1970 by Labeyrie [5], with the introduction of stellar speckle interferometry that deciphers diffraction limited spatial Fourier spectrum and image features of stellar objects by counteracting blurring effect caused by the atmospheric turbulence. This method has made impacts in several important fields in astrophysics [6, 7]. Further development in hardware technology has made it possible to compensate in real time the wavefront perturbations, particularly in infra-red wavebands [8].

Though the angular resolution capabilities in astronomy differ across the electromagnetic spectrum, it is limited with the diameter of the single aperture. The resolution improves if the baselines are extended by using diluted aperture interferometry, which combines signals to obtain information that could not be supplied by either of the signals individually. Spectacular progress has been witnessed in the case of the radio interferometry [9] in which very long baseline interferometry (VLBI) is used to obtain milliarcsecond spatial resolution. The optical interferometry using diluted aperture had been developed in 1975 by Labeyrie [10]. This had made it possible to obtain a very high resolution of the order of a few milliarcseconds. This technique has addressed subjects such as star surface imaging, close binaries, circumstellar environment. Over the years optical interferometry has slowly gained in importance and today it has become a powerful tool. Several such instruments are in operation and in some cases, large telescopes are used. The methods and technology of interferometry in infrared wavebands in atmospheric windows have also been established [11]. The progress in developing the new generation ground- and space-based optical interferometer is noteworthy. In this article, the current trend and the path to future progress in aperture synthesis techniques using large number of telescopes are elucidated.

2 Aperture mask at the telescope

The concept of aperture mask using two holes on top of the telescope was suggested by Fizeau [1]. In this technique the beams are diffracted by these sub-apertures which produce Young's fringes at the telescope's focal plane. These fringes remain visible in presence of seeing, which allow to obtain high angular measurements of stellar objects. Initial experiment by Stefan with 1 meter telescope at Observatoire de Marseille revealed that the fringes appeared within the common Airy disk of the sub-apertures. But he could not notice any significant drop of fringe visibility. Since the maximum achievable resolution is limited by the diameter of the telescope, he concluded none of the observed stars approached 0.1 arc sec. in angular size. The notable advantages of such an interferometer are: (i) the telescope acts as both collector and correlator, thus the temporal coherence is automatically obtained due to the built-in zero optical path difference (OPD), and (ii) the spatial modulation frequency, as well as the required sampling of the image change with the separation of sub-apertures. The intensity in the focal plane can be formulated as follows:

$$I(\mathbf{x}) = a(Dx) \left[I_1 + I_2 + 2\sqrt{I_1 I_2} |\gamma_B(0)| \cos \left\{ \frac{2\pi}{\lambda} \left(\frac{Bx}{f} + d \right) - \psi_B \right\} \right], \quad (1)$$

where, B is the baseline, D the diameter of the sub-apertures, f the focal length, $a(Dx)$ the image of each sub-apertures (Airy disk), ψ_B the phase of $\gamma_B(0)$, $\gamma_B(0)$ the complex degree of coherence; it measures the spatial coherence, $2\pi d/\lambda$ the incidental non-zero OPD between the fields, and d the extra optical path in front of one aperture.

Such a technique was used at the Yerkes refractor by Michelson [12] to measure the diameter of the satellites of Jupiter. Similar experiment has also been conducted by a few others in order to record the fringes [13]. Saha et al., [14] have successfully recorded fringes of several bright stars through a Fizeau mask for an exposure time of 33 msec at the Cassegrain focus of 1 meter telescope, Vainu Bappu Observatory, Kavalur, India with a 16 mm movie camera (see Figure 1). The mask had two holes of 10 cm in diameter each and separated by $d = 69.4$ cm. In order to slow down the image, a Barlow lens (double concave lens) was inserted in the $f/13$ converging beam at the Cassegrain end of the telescope. Assuming a peak wavelength of 4500\AA , the separation of the fringes is $\lambda/d = 0.130$ arcsecond. On the film, these had a linear separation of 0.035 mm thus yielding an image scale of $3.70''/\text{mm}$.

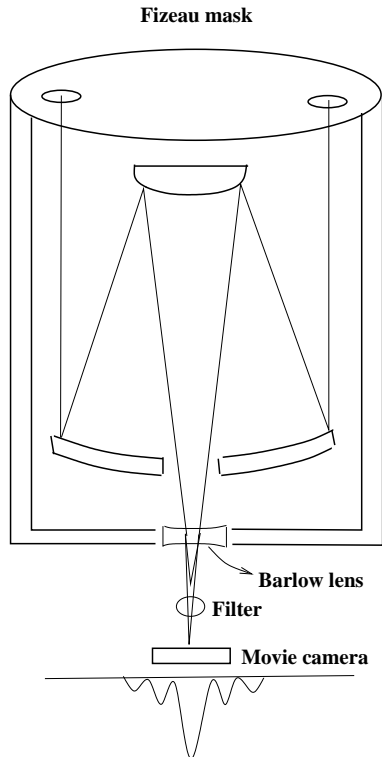


Figure 1: Fizeau mask at the 1 m telescope at Kavalur, India

The concept of using three antennae arranged in a triangle was first introduced in radio astronomy [15]. Closure-phases are insensitive to the atmospherically induced random phase errors, as well as to the permanent phase errors introduced by the telescope aberrations in optics. Since any linear phase term in the object cancels out, this method is insensitive to the position of the object but sensitive to any object phase non-linearity. The measurements of

the closure-phases was first obtained in visible band at high light level with three-hole aperture mask placed in the pupil plane of a telescope [13].

Aperture synthesis imaging technique with telescope is based on the principle of the phase-closure method. It involves observing an object through a non-redundant masked aperture of several holes and recording the resulting interference patterns in a series of short-exposure. Such a mask introduces a series of overlapping two-holes interference patterns projected onto the detector. The fringe patterns contain information about structure of the object at the spatial frequencies from which an image of the same can be reconstructed by measuring the visibility amplitudes and closure phases. This method produces images of high dynamic range, but restricts to bright objects. The instantaneous coverage of spatial frequencies is sparse and most of the available light is discarded.

3 Long baseline interferometry

The marked advantage of using independent telescopes is the increase in resolving capabilities. At radio wavelengths, development of long baseline interferometry and very long baseline interferometry (VLBI) had brought high dynamic range images with milliarcseconds resolution. Radio astronomers have produced extra-ordinary images as those of Cas A or Cyg A.

3.1 Radio interferometry

The major advantages of radio interferometry are: (i) uniform phase over individual apertures, (ii) time integration, (iii) phase stability of delay lines and (iv) electric delay lines. A radio interferometer consists of a pair of directional antennae separated by a baseline vector, \mathbf{B} , which are tuned to receive radio emissions from a distant source in a desired radio frequency (RF) band. The signals from the two receivers are then cross-correlated (multiplied and accumulated) to produce a cross-correlation ‘fringe pattern’. This fringe pattern can then be analyzed to produce an image of an astronomical object. The fringe pattern of a two element interferometer is shown in Figure (2).

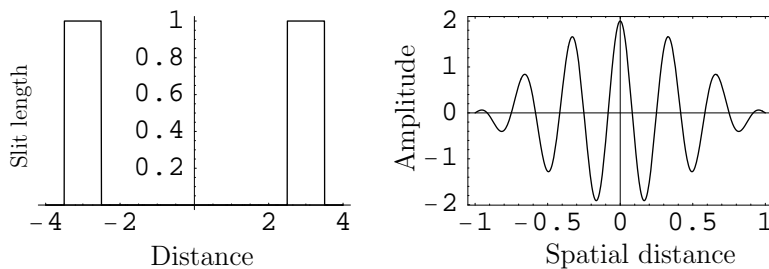


Figure 2: (a) Diagrammatic representation of slits in an interferometer, and (b) fringe pattern.

The antennae are pointed at the radio source of interest and are configured to receive the signal and process it into a form suitable for transmission to the correlator. If the antennae are in close proximity to each other (connected element interferometry), the signals are sent to the correlator and processed immediately. If the antennae are separated by long distances (Very Long Baseline Interferometry – VLBI), the signals are recorded on magnetic tape and the tapes are shipped to the correlator for processing at a convenient time.

The fringe visibility can be calculated from the variation of intensity with time. In the above figure the radio source which is to be observed is at an angle of θ . Due to this the effective baseline of the interferometer (is given by projection of the telescope positions onto a plane perpendicular to the source direction) is changed and the signal should travel an extra path of dl to reach right hand antenna (geometric delay = $dl \cos \theta/c$, in which c is speed of light). The signals from both the antennae should reach the signal intensity detector at same time. For this geometric delay is compensated using a signal delay component δt (instrumental delay).

In order to get the two dimensional map of the sky the separation of the antennae should be varied in two dimensions. The positions of the antennae are specified by its co-ordinates (a, b) and the position of the source in the sky is described using two angles θ and Φ where θ is the angle made by source with a -axis and Φ the angle with axis b . The effective baseline (x, y) will be $(a \cos \theta, b \cos \theta)$. u and v are dimensionless conjugates of θ and Φ . $u = \kappa x$ and $v = \kappa y$ where κ (wave number) = $2\pi/\lambda$ (wavelength). The complex visibility function at two points in $u - v$ plane are given by,

$$\begin{aligned} (u, v) &= (\kappa x, \kappa y) = (a\kappa \cos \theta, b\kappa \cos \Phi) \\ (u, v) &= (-\kappa x, -\kappa y) = (-a\kappa \cos \theta, -b\kappa \cos \Phi). \end{aligned} \quad (2)$$

Complex visibility function values are calculated for every point in the $u - v$ plane. Sky brightness distribution is obtained by taking the Fourier transform of the above results.

3.2 Infrared interferometry using heterodyne technique

The beam separation and heterodyne technique to reduce the high frequency signal to an intermediate one can be employed as well. The advantages of the heterodyne technique in the case of beam recombination are: a larger coherence length, a simplification of the transport of the signal from the collector to the recombiner. Like radio interferometry, infrared interferometry also uses such technique [11, 16]. Let $U_s(t)$ and $U_l(t)$, be respectively the signals of a wave coming from a star and of an artificial source (laser), which are expressed as,

$$U_s(t) = a_{s0} e^{-i[\omega_s t - \psi]}, \quad (3)$$

$$U_l(t) = a_{l0} e^{-i\omega_l t}. \quad (4)$$

The laser is the phase reference. A detector like a photodiode, illuminated by the sources (star + laser) yields an electrical signal corresponding to the light

intensity:

$$\begin{aligned}
I(t) &= |U_s(t) + U_l(t)|^2 \\
&= \left(a_{s0} e^{-i[\omega_s t - \psi]} + a_{l0} e^{-i\omega_l t} \right) \left(a_{s0} e^{i[\omega_s t + \psi]} + a_{l0} e^{-i\omega_l t} \right) \\
&= a_{s0}^2 + a_{l0}^2 + 2a_{l0} a_{s0} \cos[(\omega_l - \omega_s) + \psi].
\end{aligned} \tag{5}$$

If ω_l and ω_s are close, the frequency of I is low enough to fit in the bandwidth of the detector and its electronics (a few GHz) and I carries the phase information from the radiation of the star. By multiplying the signals I_1 and I_2 yielded by two apertures with heterodyning systems, one extracts a visibility term. However, the lasers must have the same phases for the two apertures. The first infrared long baseline interferometer, called SOIRDÉTÉ, was designed for heterodyne interferometry at 8-11.5 μm spectral range [11]. This instrument was installed at the Observatoire de Calern, France. It had ceased operation. The SOIRDÉTÉ consisted of a pair of 1 m telescopes with a 15 m East-West horizontal baseline. Beams were received in the central laboratory on a double cat's eye delay line on step by step movable carriage; natural OPD drift due to the Earth-rotation was used for acquiring fringes [17]. Two similar detectors were used in order to increase the S/N ratio and to eliminate atmospheric fluctuations. It has yielded interesting results on α Orionis.

Another similar instrument, known as IR spatial interferometer, Mt. Wilson is operating at 11 μm ; each telescope comprises of a 1.65 m parabolic mirror and 2 m flat mirror equipped with an automated guiding and tip-tilt control system at 2 μm [18]. Observations of NML Cygni, α Scorpio, as well as of changes in the dust shell around Mira and IK Tauri, [19, 20], mid-IR molecular absorption features of ammonia and silane of IRC+10216 and VY CMA [21] etc., have been made.

3.3 Optical interferometry

In Optical interferometry, two different telescopes are used to receive the signals from a distant source, and the primary mirrors are adjusted carefully. The mirrors have to be placed so as to compensate the geometrical delays as one primary mirror receives light from the distant source first. This ensures that both the light waves reach the detector at same time. The output of this is a combination of bright and dark fringes resulting from the interference of two waves. If the source is very small, then there will be a high contrast in the fringes but as the size of source increases the contrast of fringes decreases. The resolution of this method depends on the length of baseline rather than diameter of individual mirrors. This setup is, therefore, more cost effective than the large single optical telescope. The fringes which are obtained are examined and the visibility and contrast are converted using Fourier transforms (Bracewell, 1965) so that the object under observation can be mapped, and all the properties such as magnitude. This method is very useful to find the angular diameters of stars

and binary star orbits. The fringe contrast, called visibility, is given by,

$$V = \frac{I_{max} - I_{min}}{I_{max} + I_{min}}. \quad (6)$$

Figure 3 depicts the visibility curves for uniformly bright circular disks. The visibility in this case is given by,

$$V(s) = \left| \frac{2J_1(\pi as)}{\pi as} \right|, \quad (7)$$

where J_1 is the first order Bessel function.

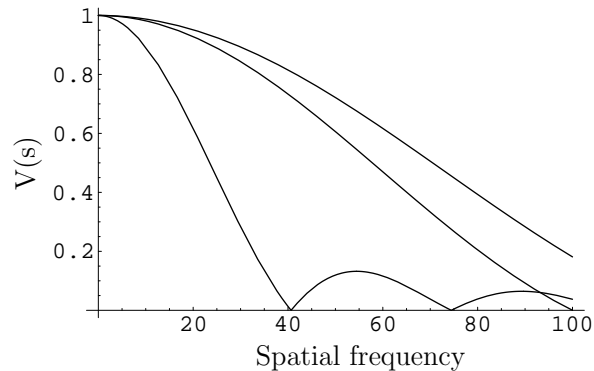


Figure 3: Visibility vs. spatial frequency.

The frequency of first zero of the function, s_0 , scales inversely with angular diameter of the source such that $a \approx 1.22/s_0$. The two major limitations of optical interferometry are atmospheric turbulence (a state of the flow of air in which apparently random irregularities occur in the air's instantaneous velocities, often producing major deformations of the flow.) and limited response time of interferometer. Due to the small wavelengths of the signals the interferometer should be fast enough to respond to them. To overcome this problem adaptive optics which consist of a number of self adjusting mirrors are used to sense the irregularity in the signal and tilt the mirror rapidly. As the number of telescopes increases the complexity of the mirror system also increases as it is necessary to compensate for the numerous beams which contribute to the interference pattern. This procedure is implemented in Keck Interferometer as well as VLTI. Optical interferometry faces many drawbacks, such as

1. many phase cells over the pupil, hence, the size of the telescope becomes limited to the size of the Fried's parameter,
2. short atmospheric coherence time; interference pattern should be detected in few milliseconds to avoid smearing due to turbulence,

3. the light from the source must be gathered within short time, or the source will move from the field of vision,
4. optical delay lines, high speed photodetectors with high-level storage and processing capabilities and frequency-stabilized lasers to measure continually changing delay line lengths,
5. mechanical stability of telescopes,
6. beam recombination (pupil or in image plane),
7. limited $u - v$ coverage, and
8. limited accuracy on amplitude and phase estimates.

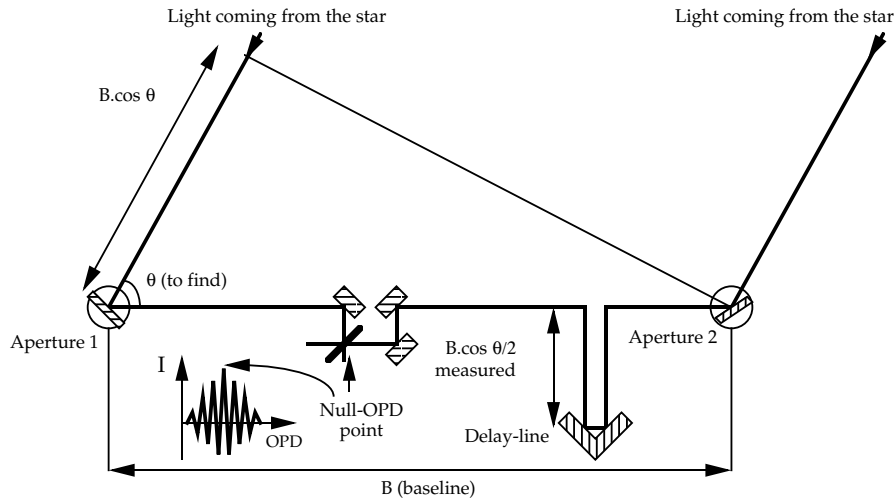


Figure 4: Principle of long baseline interferometry using two telescopes.

Labeyrie [10] extended the concept of speckle interferometry to a pair of telescopes that are run on tracks for variable North-South baseline. It combines the features of the Michelson design and the radio interferometers. These telescopes track simultaneously the same source (star) and send the collected light to the central laboratory where the star images are superposed at the foci in order to produce Young's fringes. The beams from these telescopes are recombined in an image plane after reconfiguring the pupils. Fringed speckles are visualized when a speckle from one telescope is merged with the speckle from other telescope. These fringed speckles are dispersed and the spectra are recorded at short-exposure using a photon counting detector. The beam-recombining optical devices were kept on a computer controlled motor driven carriage parallel to the baseline. This carriage moves along the telescopes to maintain constant zero OPD that changes due to diurnal motion, within the coherence length between

the two beams. Figure 4 depicts the concept of the amplitude interferometer using two independent telescopes.

The present recombiner called recombineur pour grand interféromètre (RE-GAIN) at Grand interféromètre à deux télescopes (GI2T) that comprises of a pair of 1.5 meter telescopes, uses a delay-line featuring a cat's eye reflector with variable curvature mirror. Each Coudé beam coming from the telescopes meets a pupil stabilizer, a field rotator, a wedge prism and the beam combiner [22]. The different chromatic dispersion between the two beams which occur due to the atmospheric dispersion is compensated by using for each beam two prisms that can slide on their hypotenuse, forming, therefore, a plate with adjustable thickness. This thickness is modified every few minutes, following the variation of the altitude of the observed object. The first result came out of the GI2T in 1989 in which Mourard et al. [23] reported resolving the rotating envelope of hot star, γ Cas. The star was observed with a spectral resolution of 1.5 \AA centered on $H\alpha$. This result demonstrates the potential of observations that combines spectral and spatial resolution.

Another interferometer was developed by Shao [24] at Mt. Wilson observatory, called Mark III interferometer. In this two well-separated siderostat mirrors (to divert the light from the distant object in a single direction) track the target star as the Earth rotates and direct its light into a series of mirrors. Tilt-correction mirrors adjust for disturbances caused by atmospheric turbulence. Delay lines compensate for the geometric delay so that the light in each beam that left the star at the same time arrives simultaneously at the beam splitter, which combines the two beams to produce interference fringes. Detectors are used to measure the resulting interference fringes. Both the instruments, I2T and Mark III interferometer have ceased operations.

4 Imaging interferometry

Aperture synthesis combines signals from a collection of individual antennae or telescopes to provide an image with a resolution equivalent to that of a single telescope with a size equal to the maximum distance between the individual antenna. The light collected by an array of separated telescopes yields a measure of the amplitude of the spatial coherence function of the object at a spatial frequency \mathbf{B}/λ , where \mathbf{B} is the baseline vector and λ the wavelength. In order to make an image from an interferometer, one needs to estimate of the complex visibilities over a large portion of the (u, v) plane, both the amplitudes and phases. According to the van Cittert-Zernike theorem [25], if the number of samples of the coherent function can be made large, the spatial frequency spectrum of the object can be reconstructed. The signal in the n th area due to a source of emission is expressed as,

$$V_n = a_n \cos(\omega t + \psi_n), \quad (8)$$

where a_n is the amplitude of the signal and ψ_n the relative phase of the radiation.

If these signals are added together vectorily and time averaged, the intensity of the light I_n is derived as,

$$\begin{aligned}
 I_n &\propto \frac{1}{2} \sum_{j=1}^N \sum_{k=1}^N a_j a_k \cos(\psi_j - \psi_k) \\
 &= \frac{1}{2} \sum_{j=1}^N a_j^2 + \sum_{j=1}^{N-1} \sum_{k=j+1}^N a_j a_k \cos(\psi_j - \psi_k). \tag{9}
 \end{aligned}$$

The first term of the above equation (9) is proportional to the sum of the power received by the elementary areas. The resolving power is derived from the cross product. Each term can equally be measured with two elementary areas in positions j and k . The term, $\psi_j - \psi_k$, is expressed as,

$$\psi_j - \psi_k = \frac{2\pi}{\lambda} \mathbf{B}_{jk} \cdot \mathbf{s}, \tag{10}$$

where \mathbf{B}_{jk} is the separation of the two elemental areas, and \mathbf{s} the unit vector directing to the source.

The second term on the right-hand side of the equation, describes the interference through the cross product, contains high resolution information. An image can be reconstructed from sequential measurements of all the cross products using pairs of sub-apertures. For n telescopes, there are $n(n - 1)/2$ independent baselines, with, $n - 1$ unknown phase errors. The potential of such a technique [26] in the optical domain was demonstrated by the spectacular images produced with aperture-masking of a single telescope.

A single interferometer with a fixed baseline measures one Fourier component of sky brightness within the envelope pattern of the instrument. So by sampling the source's complex visibility function at particular intervals in the baseline one can obtain brightness distribution from the Fourier transform of visibility function. Due to the Earth's rotation, the length and orientation of interferometer baseline changes. Due to this uv -plane samples in an elliptical way during a 24-hr period. A large number of ellipses can be traced by changing the interferometer spacing till source is not varying with time. The spacing between the telescopes can be changed by moving one of the telescopes along a rail track. This method is called earth rotation aperture synthesis. Arrays of telescopes connected in pairwise are called as aperture synthesis arrays.

The interferometer spacings can be filled up by fixing a linear array of telescopes and having one or more movable telescopes. The number of baselines that can be traced simultaneously with n telescopes are $n(n - 1)$. The main theme of array telescopes is to have maximum coverage of uv -plane. Large spacing results in high angular resolution. But to have continuous Fourier components all the intermediate spacings are required. The extent of this entirely depends on the design of the systems (concerning the spacings between the telescopes and shape in which they should be arranged). If the source is constant over a extent of observations, then it is not necessary that all the necessary baselines

simultaneously exist. Aperture synthesis about study of techniques of getting maximum information from data keeping in view the limitations involved in that particular method.

At optical frequencies, even more than at radio frequencies, the calibration of the imaging performance of the system is vital if high-quality images are to be obtained. This requires an assessment of the phase errors associated with each sub-aperture in the array. In astronomy, the compact and high-contrast nature of the objects imaged and the change in interferometer orientation due to the diurnal rotation of the earth permit one routinely to obtain synthetic images of great quality.

Table I
Functional components of an optical imaging array

Components	Parameters to consider
Collectors	size, number, array design
Beam transporter	free or guided
Delay compensator	vacuum or air
Beam combiners	number and nature of combiners
Detector	sensitivity, temporal and spectral resolution

The angular resolution of an interferometer entirely depends on the largest possible spacing between any two telescopes and sensitivity depends on the diameter of the telescope's objective lens. The orientation and fringe spacings can be obtained from vector spacing between the aperture pair which is generating fringes. Fringe orientation is normal to the vector and the period is equal to the length of the vector. The orientation and period of fringes are denoted by the spatial frequency (u, v) . Visibility is a measure of contrast of the fringes and phase measures the location of the fringe crest relative to the optic axis. The functional components of an optical imaging array is given in table I.

4.1 Telescope configuration

A number of telescopes are usually placed in arrays in two ways such as:

1. Phased arrays and correlator arrays; In this method, a phased array is one in which all the telescopes are connected to a single power combiner whose output is given to a square law detector. The square law detector

adds the individual voltages and gives the square of their sum as the output. On the other hand if the telescopes are connected pairwise in all possible combinations, it is called a correlator array. Phased arrays of small telescopes can be used as single elements in correlator arrays. If voltages at all telescope outputs are $v_1, v_2 \dots$. The output of the square-law detector is proportional to square of $v_1 + v_2 + \dots + v_n$, in which n is the number of telescopes. For n telescopes there are $n(n - 1)$ cross product terms which are of the form $v_m v_n$ involving different telescopes, m and n self product terms. If the signal from each telescope to the detector is of the same electrical length, the signals combine in phase when the direction of the incoming radiation is given by,

$$\Theta = \sin^{-1}(N/l_\lambda) \tag{11}$$

where N is an integer and l_λ is a spacing interval measured in wavelengths. The outputs of the correlator array are cross products of voltages of two connected telescopes. These are equal to the cross product terms of phase array. The loss of self product terms reduces the sensitivity of the correlator array by a factor of $(n - 1)/n$ in power. If n is large, it reduces to unity.

In a cross (+) shaped array aperture assume that width of arms is finite but small compared with length of the arms. The outputs of two arms go to a single cross correlating receiver, so the spatial sensitivity is a square. T-shaped array also has the same sensitivity. This is the cross correlation formed between East-West arm and half of North-South arm. The equivalence between spatial transfer function of cross and T is because for any pair of points in the aperture of a cross, for example, one on East arm and one on North arm, there is a corresponding pair on the West and South arms for which the spacing vector is identical. Thus one of the four half length can be removed with out effecting the (u, v) coverage.

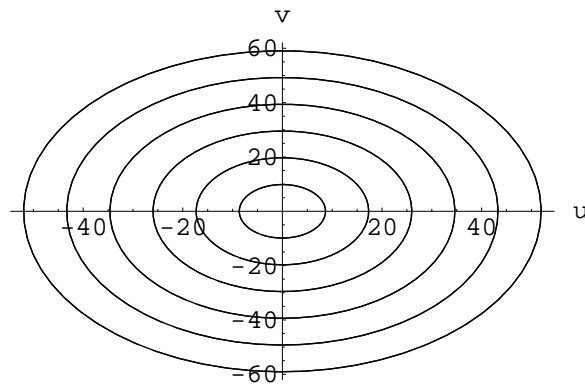


Figure 5: Linear tracking array with two elements.

2. Linear tracking arrays: In this technique, a series of ellipses are formed in uv -plane when telescopes are placed in East-West direction. The ellipses (see Figure 5) are centered at origin of (u, v) . If the spacings between the telescopes increase uniformly, these ellipses are concentric with uniform increment in their axes. If there are n telescopes, there will be $(n - 1)$ combinations of outputs with unit spacings, $(n - 2)$ combinations of outputs the unit spacings and so on.

4.2 Imaging interferometers

In order to measure the closure phase together with the measurements of visibility amplitude, it is required to have three or more telescopes. This technique has been successfully implemented by Baldwin et al. [27] in the visible band by reconstructing an image of an object using Cambridge optical aperture-synthesis telescope (COAST).

Two interferometers, namely (i) Keck interferometer [28], and (ii) Very large telescope interferometer [29] are of heterogeneous nature. They consist of large- and medium-sized outrigger telescopes. Recombining large and small telescopes is a difficult task since the signal-to-noise ratio is determined by the smaller ones. For imaging in the case of the former, the main telescopes are used with outriggers to fill in incomplete parts of the (u, v) plane. It combines phased pupils provided by adaptive-optics for the main telescopes and fast tip/tilt correction on the outriggers. While in the case of the latter, beams are received from the movable telescopes in a central laboratory for recombination and are made to interfere after introducing suitable optical delay-lines. Coudé beams from these apertures are sent through delay-lines operating in rooms at atmospheric pressure but at accurately controlled temperature.

The interferometers with two apertures cannot recover the complex visibility, but a different kind of interferometer called Large Binocular Telescope (LBT) that is being developed, can provide such a visibility. This instrument will utilize both 8.4-m primary mirrors with a baseline of 22.8 meters. These primary mirrors fitted with adaptive optics systems (AO) are co-mounted on a fully steerable alt-az mounting, thus information in (u, v) -plane can be continuously combined or coadded. The LBT AO system will employ two 91-cm diameter 1.7-mm thick f/15 secondary mirrors with 672 actuators on each mirror operating at 900 or 1000 Hz [30]. This AO system can be used for imaging and/or for nulling interferometric imaging. The nulling interferometric imaging technique based on Ronald Bracewell's nulling experiments that were first done at radio wavelengths, is under development. By nulling, faint objects such as extra-solar planets may be detectable around bright stars. The effect of nulling will suppress a bright star by a factor of $\sim 10^4$ or 10^5 . The expectations are that Jupiter-sized planets may be detectable via nulling, orbiting nearby stars, i.e., those within 20-30 light years. Also, the detection of extended protoplanetary disks should also be possible.

5 Concluding remarks

Interferometry has the advantage of being cost effective, at the same time giving very high resolution of distant objects in the sky. The radio interferometers in use have led to several new discoveries. Optical interferometry, though a relatively new field, also has some new findings to its credit. The technological advancement made it possible to witness the speedy progress of optical interferometry using diluted apertures. The new generation interferometers with phased arrays of multiple large sub-apertures would provide larger collecting areas and higher spatial resolution simultaneously. With these interferometers, many secrets of the universe will be unveiled. An important fundamental problem that can be addressed with these instruments fitted with complete AO systems is the origin and evolution of galaxies. They would be able to provide imaging and morphological informations on the faint extragalactic sources such as, galactic centers in the young universe, deep fields, and host galaxies.

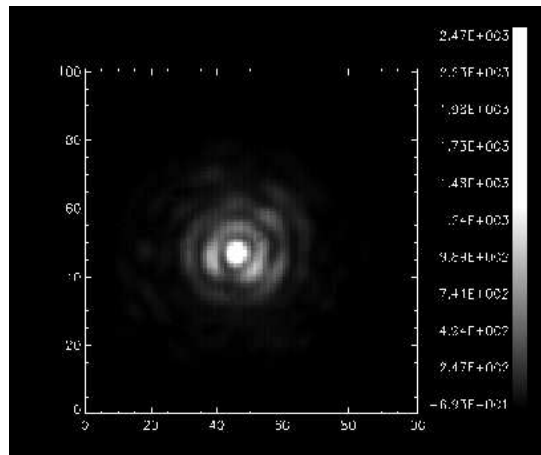


Figure 6: Laboratory simulated fringes of a binocular telescope with 17 meter baseline (Courtesy: P. Wehinger).

Though the baseline of a binocular telescope is limited, in order to cope with the present day development in the field of optical interferometry, it is necessary to take a venture of developing such an instrument in India. With a pair of 6.5 meter primary mirrors fitted with AO system, this interferometer would provide $0.014''$ resolution at a baseline of 17 meter. Figure 6 depicts the laboratory simulated image from such an instrument.

Acknowledgment: I express my gratitudes to Dr. P. Wehinger for providing the laboratory simulation of binocular telescope image and to Prof K. R. Subramanian for the discussions.

References

1. Fizeau H., Prix Borodin: Rapport sur le concours de l'année, 1867, *Comptes Rendus de l'Académie des Sciences, Paris*, 66 (1868), 934.
2. Michelson A., and Pease F., Measurement of the diameter of alpha Orionis with the interferometer, *Astrophys. J.*, 53 (1921), 249.
3. Hanbury Brown R., and Twiss R. Q., A test of an intensity interferometer on Sirius A, *Proc. Roy. Soc. A.*, 248 (1958), 222.
4. Hanbury Brown R., *The intensity Interferometry, its Applications to Astronomy*, (1974), Taylor & Francis, London.
5. Labeyrie A, Attainment of diffraction limited resolution in large telescopes by Fourier analysing speckle patterns in star images, *Astron. Astrophys.*, 6 (1970), 85.
6. Saha S K, Emerging Trends of Optical Interferometry in Astronomy *Bull. Astron. Soc. Ind.*, 27 (1999), 443.
7. Saha S K, Modern Optical Astronomy: Technology and Impact of Interferometry, *Rev. Mod. Phys.*, 74 (2002), 551.
8. Roddier F (editor), *Adaptive Optics in Astronomy*, (1999), Cambridge Univ. Press.
9. Furke B. F., and Graham-Smith, F., 2002, An Introduction to Radio Astronomy, Cambridge University Press, UK.
10. Labeyrie A, Interference fringes obtained on VEGA with two optical telescopes, *Astrophys. J.*, 196 (1975), L71.
11. Gay J, and Mekarnia D, Infrared interferometry at CERGA, *Proc. ESO-NOAO conf.* ed., F. Merkle, ESO, FRG, 811.
12. Michelson A., Measurement of Jupiter's satellites by interference, *Nature*, 45 (1891), 160.
13. Baldwin J, Haniff C, Mackay C, and Warner P, Closure phase in high resolution optical imaging, *Nature*, 320 (1986), 595.
14. Saha S K, Venkatakrishnan P, Jayarajan A, and Jayavel N, Astrophotography with High Angular and Temporal Resolution: Preliminary Results from the Kavalur Experiments, *Current Sci.*, 56, (1987), 985.
15. Jennison R C, A phase sensitive interferometric technique for the measurement of the Fourier transforms of spatial brightness distributions of small angular extent, *Mon. Not. R. Astron. Soc.*, 118 (1958), 276.
16. Townes C. H, Bester M, Danchi W, Hale D, Monnier J, Lipman E, Everett A, Tuthill P, Johnson M, and Walters D, Infrared Spatial Interferometer, *Proc., SPIE*, 3350 (1998), 908.
17. Rabbia Y, Mekarnia D, and Gay J, Infrared interferometry at Observatoire de la Cote d'Azur, France, *Proc., SPIE*, **1341**(1990), 172.
18. Lipman E A, Bester M, Danchi W C, and Townes C H, Near-infrared guiding and tip-tilt correction for the UC Berkeley Infrared Spatial Interferometer, *Proc., SPIE*, **3350**(1998), 933.
19. Glinski R J, Lauroesch J T, Reese M D, and Sitko M L, Temperature and Velocity Diagnostics of the Red Rectangle from Ultraviolet Spectra of CO and C I, *Astrophys. J.*, 490 (1997), 826.

20. Lopez B, Danchi W C, Bester M, Hale D S, Lipman E A, Monnier J D, Tuthill P G, Townes C H, Degiacomi C G, Geballe T R, Greenhill L J, Cruzalébes P, Lefèvre J, Mékarnia D, Mattei J A, Nishimoto D, and Kervin P W, Nonspherical Structures and Temporal Variations in the Dust Shell of o Ceti Observed with a Long Baseline Interferometer at 11 microns, *Astrophys. J.*, **488**(1997), 807.
21. Monnier J D, Danchi W C, Hale D S, Tuthill P G, and Townes C H, Mid-Infrared Interferometry on Spectral Lines. III. Ammonia and Silane around IRC +10216 and VY Canis Majoris, *Astrophys. J.*, **543**(2000), 868.
22. Rousselet-Perraut K, Vakili F, and Mourard D, Polarization effects in stellar interferometry, *Opt. Eng.*, 35 (1996), 2943.
23. Mourard D., Bosc I., Labeyrie A., Koechlin L., and Saha S, The Rotating Envelope of the Hot Star Gamma Cassiopeia Resolved by Optical Interferometry, *Nature*, 342 (1989), 520.
24. Shao M., Mark III interferometer and its successor, Proc. ESO-NOAO conf. 'High Resolution imaging Interferometry', ed., F. Merkle, (1988), 823.
25. Born M, and Wolf E, *Principles of Optics*, (1984), Pergamon Press.
26. Tuthill P G, Monnier J D, Danchi W C, Wishnow E H, and Haniff C A, Michelson Interferometry with the Keck I Telescope, *Pub. Astron. Soc. Pac.*, 116 (2000), 2536.
27. Baldwin J., Boysen R, Haniff C, Lawson P, Mackay C, Rogers J, St-Jacques D, Warner P, Wilson D, and Young J, Current status of COAST, Proc., *SPIE.*, 3350 (1998), 736.
28. Colavita M M, Boden A F, Crawford S L, Meinel A B, Shao M, Swanson P N, van Belle G T, Vasist G, Walker J M, Wallace J P, and Wizinowich P L, Keck Interferometer, Proc., *SPIE.*, 3350 (1998), 776.
29. Derie M, Brunetto E, Duchateau M, Amestica R, and Aniol P, VLTI test siderostats: design, development, and performance results, Proc., *SPIE.*, 4006 (2000), 99.
30. P Wehinger, *Private Communication* (2004).